
Article:
Revin, D. and Matcher, S. (2022) Fast-sweeping continuous wave quantum cascade laser operating in an external cavity with polygon mirror. Optics Express, 30 (12). pp. 21843-21853. ISSN: 1094-4087

https://doi.org/10.1364/oe.453045

Research Article Vol. 30, No. 12 / 6 Jun 2022 / Optics Express 21843
Optics EXPRESS

Fast-sweeping continuous wave quantum cascade laser operating in an external cavity with polygon mirror

DMITRY G. REVIN[1,2] AND STEPHEN J. MATCHER[1,3]

[1]Department of Electronic and Electrical Engineering, The University of Sheffield, Sir Frederick Mappin Building, Mappin Street, Sheffield, S1 3JD, United Kingdom
[2]d.revin@sheffield.ac.uk
[3]s.matcher@sheffield.ac.uk

Abstract: We report a continuous wave room temperature quantum cascade laser operating in an external cavity in the Littrow configuration with a 10-facet polygon mirror rotating at 24,000 RPM. The quantum cascade laser emission is swept across ~1520 - 1625 cm^{-1} wavenumber range in less than ~45 µs with a sweep repetition rate of 4 kHz. The measured maximum output power at the laser gain maximum, 15°C and 0.86 A driving current is ~90 mW; the estimated average output power across the 45 µs wavenumber sweep is ~50 mW. Through its sweep, the laser emits on the sequential Fabry-Perot longitudinal modes of the laser chip cavity with the mode separation of ~0.5 cm^{-1}. The linewidth of the emitting modes is less than ~0.05 cm^{-1}. Spectral measurements of the infrared absorption features of a 10 µm thick layer of acetophenone and water vapor in the air have demonstrated the capability of obtaining spectral data in less than 45 µs.

1. Introduction

The development of tunable mid-infrared sources based on quantum cascade lasers (QCLs) is an active area of research driven by their spectroscopic applications. Tunable QCLs acquire spectra using a single element detector and a compact source, which is advantageous compared to broad-band emitter technologies such as supercontinuum sources. Mid-infrared laser absorption spectroscopy has already been developed and successfully used in areas such as medical breath analysis, monitoring of industrial processes, and sensing of environmental pollutants. These applications involve relatively slow changing processes and the speed at which the data must be collected does not require a very fast tunable source. However, in some more recent areas of research, for example, monitoring of transient chemical real-time reactions and in-line process analysis [1,2], combustion diagnostics in turbulent environment [3], single shot stand-off detection [4] and mid-infrared optical coherence tomography (OCT) [5,6], a source with a broad spectral range and sub-milli-seconds wavelength tuning capability is in great demand.

QCL are versatile and powerful laser sources covering the full mid-infrared (~3 - 20 µm) wavelength range. Traditionally, the QCL wavelength tuning has been achieved in two ways. Distributed feedback (DFB) QCLs [7] have high continuous-wave (CW) output power, a narrow linewidth, but a very limited wavelength tuning range of a few cm^{-1} via temperature or driving current tuning. These lasers are perfectly suitable for detection of a gaseous sample targeting a single narrow absorption line but lose their usefulness for broadband applications and multi-species detection. Arrays of several DFB lasers [8], fabricated for several emitting central lines, demonstrated a much-improved combined tunability over 200 cm^{-1} [9], however, the manufacturing process is excessively difficult and expensive. As an alternative to DFB lasers,

#453045 https://doi.org/10.1364/OE.453045
Journal © 2022 Received 7 Jan 2022; revised 4 Mar 2022; accepted 11 Mar 2022; published 2 Jun 2022

Optics EXPRESS

QCLs operating in an external cavity configuration [10] have become widely utilized and reliable sources with broadband tunability, that can now reach more than 400 cm^{-1} [11]. The tuning is obtained by rotating either a diffraction grating or a mirror in the external cavity. However, mode-hop free tuning, limited to only ~1 cm^{-1} of range, was achieved by a mode tracking system, where the laser current and the external cavity length are modulated during the tuning process [12]. Early external cavity laser systems had a diffraction grating attached to a stepper motor and the tuning speed was relatively slow, which is a big limiting factor for applications requiring sub-millisecond measurement time, such as mid-infrared OCT, combustion/ explosion diagnostics and hyperspectral imaging. A tuning rate of 5 kHz for an external cavity QCL system with a mechanical grating and a mirror was demonstrated by fast piezo-driven tilting of a small intracavity mirror, however with a tuning range limited to ~7 cm^{-1} [13]. For a micro-opto-electro-mechanical system (MOEMS) scanning mirror the reported tuning rate is 6 kHz with a higher tuning range of ~170 cm^{-1} [14]. As an alternative approach, the fast tilting of a MOEMS grating was used, resulting in a scanning rate of 1 kHz [1]. Another approach to control the angle of the intracavity mirror is to use a galvanometer scanner [15,16], however, the maximum reported tuning rate is less than ~400 Hz. Lyakh et al. [17] suggested and successfully implemented an acousto-optic modulator to provide optical feedback for external cavity QCLs. The authors reported currently the fastest sweep time, ~16 µs, for a tuning range of ~70 cm^{-1}, operating in the CW regime. However, the resolution of their system is relatively low, with the linewidth of the laser emission being ~1.5 cm^{-1} for CW operation and ~4.5 cm^{-1} for the quasi-CW operation, which could be a limitation for some applications such as mid-infrared OCT (where a broad emission line results in a strong axial roll-off in sensitivity) or the detection of gases. Despite the impressive results, the commercial implementation of the system has arguably not yet reached maturity.

Most of the present fast-sweeping external cavity laser systems operate in the pulsed regime, so the emission line is inherently broadened due to the chirped current effect. Recently, a CW fast swept-wavelength external cavity QCL with a tuning range of 135 cm^{-1} has been demonstrated with the scanning galvanometer in the Littman-Metcalf cavity geometry [18] but with a tuning rate of only 100 Hz and a resolution less than 0.5 cm^{-1}.

In this paper, we demonstrate a high CW power fast swept external cavity QCL with a rotating polygon mirror and a stationary diffraction grating in the Littrow configuration. The polygon scanning mirror has already been widely used in fast swept external cavity laser systems operating in the near infrared range [19], but, to our knowledge, has not been reported yet for a mid-infrared laser system.

2. Experimental section

The CW-FP-6.3 continuous wave QCL gain chip was supplied by Alpes Lasers SA, Switzerland. The chip has a gain maximum at ~1570 cm^{-1} and is a buried heterostructure with the width of 10 µm and the length of 3 mm, soldered onto an AlN tile and a small gold-plated copper submount. The chip has one facet left as-cleaved whereas the other facet, directed towards the external cavity, is anti-reflection coated. Subsequently, the chip on the submount was attached to an in-house-built copper mount positioned on a thermo electric cooler (TEC) to monitor the laser operating temperature. The submount temperature was kept at 15°C and the hot side of the TEC was water cooled. Light was coupled into and out of the chip using two #390010 (LightPath Technologies, USA) short effective focal length (1.47 mm) short working distance (~0.63 mm) high numerical aperture (NA = 0.83) aspheric lenses, which were aligned in their housings and attached to the in-house-built laser mount. To keep the alignment of the two collimating lenses steady and independent of ambient temperature variations, the housings holding the lenses were attached to the same in-house-built copper mount resulting in the same operating temperature for both the laser and the lenses. The in-house-built mount was positioned on a pitch-yaw adjustable

Optics EXPRESS

stage and was rotated 90 degrees around the emission direction of the laser chip to ensure the emitted electric field is polarized in the plane of the optical bench. The collimated laser beam from the anti-reflection-coated facet is directed towards a polygon mirror (~55 mm away from the lens) whose optical axis of rotation lies perpendicular to the surface of the optical bench (Fig. 1). The 62 mm diameter polygon mirror has 10 facets, each with a clear aperture of 4.7 mm (height) by 19.7 mm (width). The rotation of the polygon mirror is controlled by a SOS-SA24C 6,000-24,000 RPM polygon scanner (Cambridge Technologies, USA). The rotating laser beam reflected from the polygon mirror is directed onto a Thorlabs GR2550-30035 stationary diffraction grating (Littrow configuration) with a useable aperture of 25 mm (height) by 50 mm (width), 300 grooves/mm (the grooves are perpendicular to the surface of the optical bench) and average efficiency of ~80% (in the ~1520 - 1625 cm^{-1} range) for an incident light with polarization perpendicular to the grating grooves. An external cavity is thus formed between the diffraction grating and the uncoated laser facet. Since the laser beam spot on the diffraction grating is changing its position during the rotation of the polygon mirror, the overall length of the laser external cavity is also changing from ~75 mm to 120 mm.

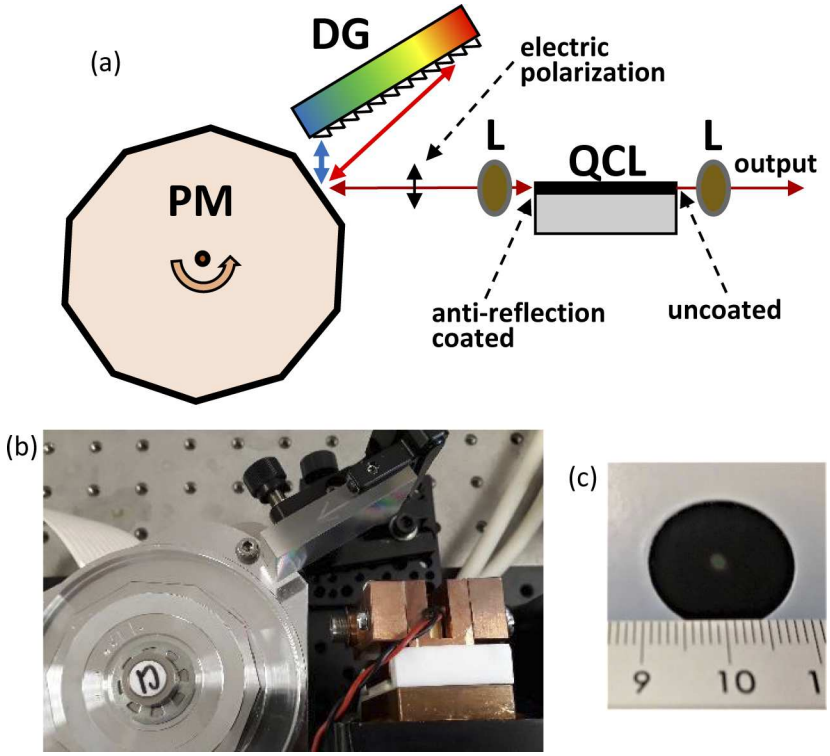

Fig. 1. Schematic diagram (a) and the photo (b) of the external cavity QCL with a polygon mirror. PM – rotating polygon mirror on a scanner, DG – fixed position diffraction grating in the Littrow configuration, QCL – quantum cascade laser gain chip on a submount, L – achromatic lenses. The DG and the uncoated laser chip facet form the cavity end mirrors. Laser electric polarization is perpendicular to both the rotation axis of the polygon mirror and to the direction of the diffraction grating grooves. (c) Photo of the laser beam spot on a liquid crystal film infrared card at the distance of ~35 cm away from the laser.

The laser output was characterized by a thermo-electrically cooled PVMI-4TE-8-1×1 detector (Vigo System S.A., Poland) with a time constant better than 4 ns. To avoid saturation of the detector, various neutral density free-standing metal grid filters (Lasnix, Germany) were used

Optics EXPRESS

before the detector. The detector output signal was processed by a 12-bit, 2 channels, 1 kS/s - 500 MS/s ATS9350 waveform digitizer (AlazarTech. Inc., Canada). The comparative spectral measurements were conducted on a non-purged Nicolet iS50 Fourier Transform Infrared (FTIR) Spectrometer with a room temperature deuterated triglycine sulphate (DTGS) detector.

To provide a triggering signal for the digitizer, a start-of-scan detector kit (Precision Laser Scanning, LLC, USA) was introduced. This kit includes a generic low power red diode laser and a fast, small-size detector. To ensure precise time synchronization the red laser beam is directed onto the same polygon mirror facet which is utilized for the external laser cavity, and the reflected, rotating red laser beam synchronously hits the detector creating short triggering pulses with a rise time less than 7 ns. Careful positioning alignment of the start-of-scan scheme was required to ensure the right timing of the triggering pulses relative to the start of the sweep of the external cavity laser.

The laser operates only when optical feedback is provided by the external cavity, with the CW laser threshold of ~0.57 A. If the external cavity is shut then the laser does not emit up to, at least, ~0.86 A, the maximum operating current used in this set-up. CW output power at the wavelength corresponding to the peak of the laser gain was calibrated by a S401C thermal power sensor (Thorlabs) for the polygon mirror being stationary. It was found to be ~90 mW at the driving current of 0.86 A, the supplied voltage of 10.38 V and 15°C heat-sink temperature. The overall laser performance (ability to operate in CW regime, laser output power, the gain range) is mainly defined by the present laser gain chip and can be improved further with future development of QCL devices.

3. Results

3.1. Wavelength tuning

The anticlockwise rotation of the polygon mirror (the only possible direction for this scanner) for the orientation of the diffraction grating as shown in Fig. 1, results in a change in the incident angle (on the grating) from ~ 80.7 to 67.4 degrees and a wavelength sweep from ~6.58 to 6.15 µm (1520 to 1625 cm^{-1}). The width of the diffraction grating and its proximity to the polygon mirror (~20 mm) is just enough for the laser beam to sweep across the full length of the grating to cover the gain range of the present laser, but for a QCL gain chip with a wider gain range a wider diffraction grating will be required. A liquid crystal film infrared card was used to visualize the spatial position of the output laser beam and to estimate its shape. It was found that the laser emits in a fundamental lateral mode with low divergence of the beam, which is still less than ~2 mm at the distance of ~35 cm away from the laser output lens (Fig. 1(c)). Such a beam results in a ~6 - 7 mm laser spot length on the inclined diffraction grating and a filter resolution of ~1 cm^{-1}.

The laser output power detected in time at the sampling rate of 125 MS/s (8 ns) for the driving current of 0.86 A, is presented in Fig. 2(a) (shown for four consecutive sweeps) and Fig. 2(b) (a single sweep). The sweep repetition rate of the swept laser is 4 kHz (the polygon mirror is rotating at the speed of 24,000 RPM) and a full sweep is completed in ~45 µs (the lasing duty cycle is ~18%). The average output power of the laser through a single laser sweep was estimated to be ~50 mW i.e., ~9 mW when averaged over 1 second. Through the rotation of the polygon mirror, the angle $\theta(t)$ incident on the diffraction grating is varied linearly in time t. However, both the wavelength $\lambda(t)$ and the wavenumber $\nu(t) = 1/\lambda(t)$ of the diffracted light vary non-linearly in time, leading to the observed asymmetrical shape of the laser emission vs time, which is different to that expected for a symmetrical laser gain profile. For first order diffraction and the Littrow configuration, the wavenumber is equal to $\nu(t) = 1/(2\ d\ \mathrm{Sin}(\theta(t)))$, where d is the diffraction grating pitch size. Consequently, emission was re-sampled, from being uniformly sampled in time to uniformly sampled in wavenumber. The re-sampled spectrum, averaged over 4000 sweeps (1 second), is presented in Fig. 2(c). The wavenumber sweeping range (~1520

Optics EXPRESS

- 1625 cm^{-1}) was obtained by calibration for the positions of the absorption dips of the water vapor in the air, clearly seen through the laser sweep dependence. The water vapor transmission spectrum, measured with the resolution of 0.125 cm^{-1}, for the ambient water vapor inside of the FTIR spectrometer, is also presented in the top part of Fig. 2(c) as a reference.

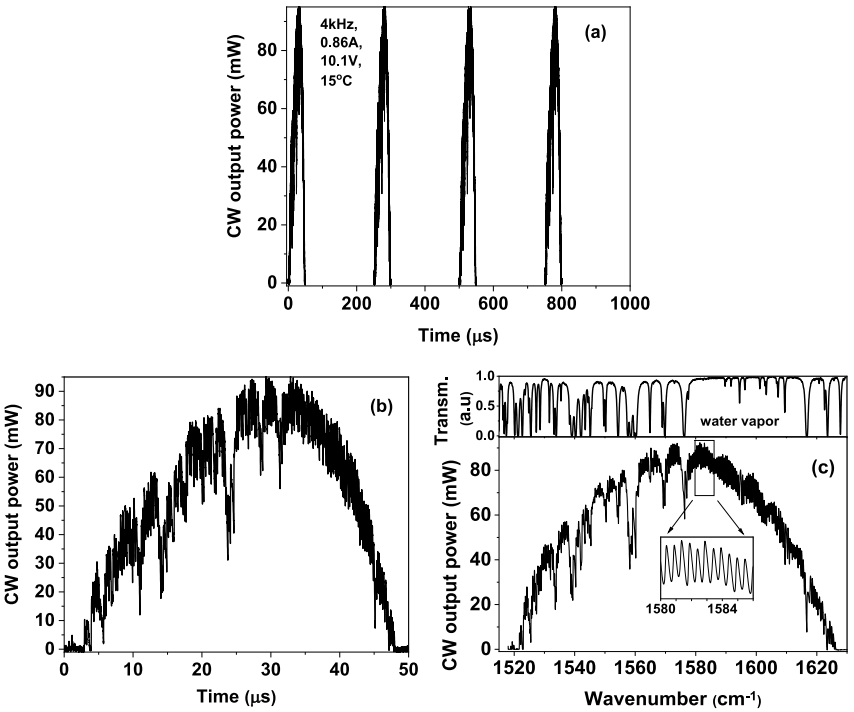

Fig. 2. (a) The external cavity laser output in time (shown for four consecutive sweeps) digitized only when the laser emits light. The polygon mirror (with 10 facets) rotates at a speed of 24,000 RPM (4 kHz repetition rate). The CW driving current is 0.86 A and the heat-sink temperature is 15°C. The laser power is attenuated by −15 dB. (b) Only a single sweep shown, for clarity. (c, lower) Re-sampled from (b) and averaged over 1 second (4000 sweeps). (c, upper) Spectrum for the water vapor transmission, as a reference. (c, inset) ~0.5 cm^{-1} mode hops.

The water absorption is not the only factor that affects the smoothness of the laser output. Clearly visible, regular changes of the laser intensity are associated with the mode hops. In an ideal situation, the laser would operate on the closely positioned (by the energy of ~ 0.04 - 0.06 cm^{-1}) longitudinal modes defined by the external cavity, formed between the diffraction grating and the uncoated laser facet. Unfortunately, the present anti-reflection coating on the coated laser facet is not perfect and it is estimated to have ~1 - 2% remaining reflectivity and because of that an additional resonator cavity (the laser chip cavity) is formed inside the external cavity.

The competition between these two sets of resonator modes causes the laser not to tune between successive modes of the external cavity resonator but to tune between successive Fabry-Perot (FP) longitudinal modes of the laser chip cavity (see the inset in Fig. 2(c)). The length (3 mm) and the refractive index (n ~ 3.2) of the laser chip dictate the mode separation of ~0.5 cm^{-1}. Moreover, the present resolution of the diffraction grating (~1 cm^{-1}) is not enough to distinguish between the modes of the external laser cavity but is enough to support CW laser emission for only one FP longitudinal mode of the laser chip cavity at a time.

Optics EXPRESS

Since the concentration of atmospheric water vapor constantly fluctuates inside the external cavity, the time of the switching between the emitting FP modes positioned near the water absorption lines is not very stable from sweep to sweep. Where the influence of the water absorption is not so strong the timing of mode hops is highly repeatable. Clearly resolved mode hops are still present on the average over 4000 sweeps (see Fig. 2(c)), which indicates high level of the time synchronization between the start-of-scan acquisition triggering signal and the laser sweep.

Repositioning the diffraction grating (Fig. 1(a)) into its mirror image, to reverse the direction of the wavenumber sweep from 1520 - 1625 cm^{-1} to 1625 - 1520 cm^{-1}, makes no noticeable difference in the overall performance of the external cavity QCL (see Fig. 3). This contrasts with previous reports on polygon-scanned near infrared swept lasers for OCT. In those lasers, a marked improvement in sweep repetition rate and achievable relative intensity noise is found when the cavity is tuned from short to long wavelengths (see, for example, [20]). The effect is ascribed to non-linear processes easing the transition from a bluer mode to a redder one, but not vice-versa [21]. However, in a QCL, emission occurs between electron subbands, which have a much faster gain recovery time compared to interband transitions that are utilized in near infrared lasers. For that reason, and because our external cavity laser has a larger cavity mode spacing and slower sweep repetition rate, the effect of changing direction of the wavenumber sweeping may become much less noticeable. A small discrepancy in the tuning range for the sweeps in the opposite directions (Fig. 3(a)) is because of the slight difference in the optical alignment of the external cavities.

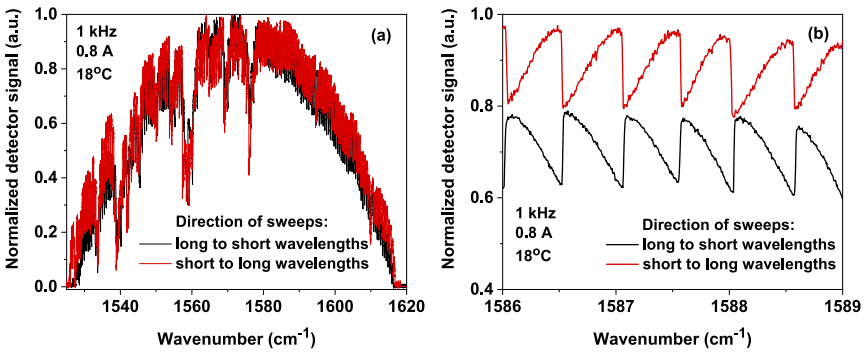

Fig. 3. (a) Normalized detector signals for a single sweep of the external cavity laser in two directions: from long to short wavelengths and from short to long wavelengths. The polygon mirror is rotating at the speed of 6,000 RPM (1 kHz sweep repetition rate). The CW driving current is 0.8 A and the heat-sink temperature is 18°C. The laser power is attenuated by −15 dB. (b) The mode hops zoomed-in from (a). The black curve is vertically shifted down, for clarity.

To estimate the linewidth of the laser emitting lines and the sweep-to-sweep wavenumber stability a Michelson interferometer was built with our external cavity laser as a source. A 5-mm thick CaF_2 BSW520 beam splitter from Thorlabs was used to split the laser beam between the two arms of the interferometer. Sweeping the laser wavenumber results in the appearance of interferogram fringes, with the oscillation frequency dependent on the optical path difference (OPD) between the interferometer arms (see Fig. 4(a) for OPD = 2 mm). To assess the laser coherence length, one of the interferometer mirrors was moved step-by-step away from the position of zero optical path difference and the peak-to-peak intensity of the interferogram fringes (for both a single sweep and the average over 1000 sweeps) was recorded for each mirror position; the resulting curves were then fitted with Gaussian curves (see Fig. 4(b)). The maximum distance (26 mm i.e., OPD/2) by which the mirror was moved has a restricted range due to limitations of

Optics EXPRESS

the current set-up. The coherence length, estimated as the Full Width at Half Maximum (FWHM) of the fitted Gaussian curves, is ~ 100 mm (for a single sweep) and ~ 90 mm (for the average over 1000 sweeps). Such a coherence length translates to the linewidth of better than ~ 0.044 (0.049) cm^{-1} [22] for each emitting line. The obtained linewidth is much narrower compared to other kHz-rate-swept QCLs and can be very beneficial for high-axial-depth OCT systems. To estimate standard deviation of the sweep-to-sweep wavenumber repeatability, the phase variances of the interference fringes have been calculated across 1000 consecutive wavenumber sweeps for the following OPD values: 2, 4, 6, and 10 mm. It was found that the phase variance values are: ~ 1.73, 3.9, 15, and 36.3 degrees squared, correspondingly, which leads to the average standard deviation for the emitting wavenumbers from sweep to sweep of ~ 0.018 cm^{-1}. In other words, the precision (i.e., jitter) of the time synchronization between start-of-scan trigger signal and a wavenumber sweep is better than 8 ns. This is comparable to the typical delay between trigger signal and the (asynchronous) Analogue-Digital-Converter sample clock, at the specified acquisition rate of the digitizer (125 MS/s).

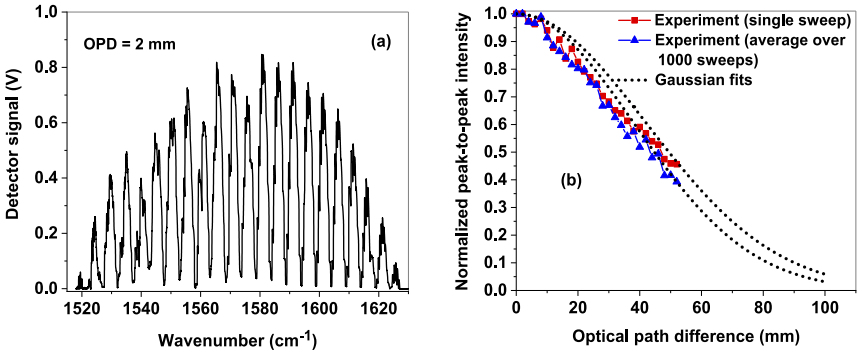

Fig. 4. (a) Interferogram fringes detected by the Michelson Interferometer, with the polygon mirror rotating at 6,000 RPM (1 kHz sweep repetition rate), re-sampled for uniform wavenumber sampling, and averaged over 1 second. The optical path difference is 2 mm. The CW driving current is 0.86 A and the heat-sink temperature is 15°C. The laser power is attenuated by −12 dB. (b) Normalized peak-to-peak intensity of the interference fringes (measured in the range of ~1580 - 1600 cm^{-1}) vs optical path difference between the interferometer arms for a single sweep and for the average over 1000 sweeps. Dotted lines: the best-fit Gaussian curves.

3.2. *Laser spectra*

The emission spectrum of the external cavity swept laser was measured with the FTIR spectrometer in a rapid scan mode with a resolution of 0.125 cm^{-1} (see Fig. 5). The transmission spectrum for water vapor in air is shown in the same figure as a reference. The influence of the water vapor absorption on the detected emission spectrum of the external cavity laser is much stronger compared to the data in Fig. 2, because of the longer distance from the external cavity laser, through the un-purged spectrometer, and onto the DTGS detector. The data on the magnified part of the laser emission spectrum (Fig. 5(b)) clearly demonstrates that the spectrum consists of narrow (with FWHM of ~0.15 cm^{-1}, limited by the FTIR resolution) lines separated by ~0.5 cm^{-1}, with their intensities strongly reduced at the wavenumbers corresponding to the water vapor absorption features. A resolution of ~0.5 cm^{-1} is more than enough for spectroscopic applications involving liquids, solids, and higher-pressure gases. On the other hand, if an absorption feature of a sample is narrower than 0.5 cm^{-1} then the emission lines of the present laser can be finely tuned to overlap with it by a slight adjustment of the laser driving current and/or the laser operating temperature.

Optics EXPRESS

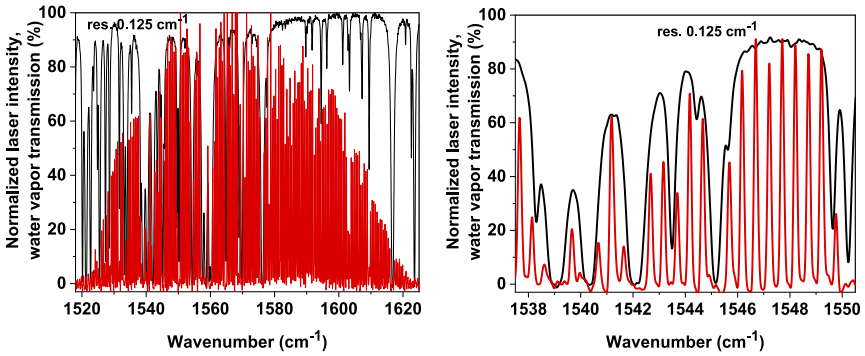

Fig. 5. (a) The normalized emission spectrum of the external cavity QCL (red) with the polygon mirror rotating at the speed of 24,000 RPM (resulted in 4 kHz sweep repetition rate), measured with an FTIR spectrometer with a resolution of 0.125 cm^{-1}. The CW driving current is 0.8 A and the heat-sink temperature is 16°C. The spectrum of the water vapor transmission (black) is shown for reference. (b) The emission spectrum of the external cavity QCL shown only in the ~1538 - 1550 cm^{-1} range to make the narrow lines of the laser emission more visible.

3.3. *Spectroscopic measurements*

To demonstrate the capability of the present swept laser for fast spectroscopic measurements and to evaluate the extent of the problem of the relatively high laser intensity noise, the transmission through a thin film (~10 μm thick) of acetophenone liquid was acquired as an example by both the swept laser (through a single ~45 μs sweep) and the FTIR spectrometer (over several seconds i.e., a factor of 10^5 longer), whose resolution was set to 0.5 cm^{-1} for comparison. Acetophenone, in the liquid phase, has two strong absorption dips in the range of ~1520 - 1625 cm^{-1} [23]. A small amount of acetophenone was pressed down between two 5-mm thick CaF_2 wedged windows, forming a transmission cell, with the distance between the windows controlled by spacers made of a 10 μm thick aluminum foil. The swept laser output beam was attenuated by −14 dB and split by a BSW520 CaF_2 beam splitter. The transmitted part of the beam was directed through the transmission cell and onto the first PVMI-4TE-8-1×1 detector, whereas the reflected part of the beam was directed onto the second PVMI-4TE-8-1×1 detector. The signal from the second detector was digitized at the same time as the signal from the first detector and used as a reference signal. Prior the transmission measurements, both detectors were calibrated for the mismatch in their responses, non-linearities and for possible difference in the distance between the laser output and the detectors, resulting in the different strength of the water vapor absorption features in the detector signals. The transmission spectra of a ~10-μm thick acetophenone liquid film are presented in Fig. 6. The red curve is the spectrum obtained in the ~45-μs sweeping time by the external cavity QCL. The black curve is the spectrum measured by the FTIR spectrometer, over several seconds of time. Similar to what was previously reported [23], there are three dips in both transmission spectra: a weak one at ~1543 cm^{-1} and two stronger ones at ~1583 and ~1599 cm^{-1}. The relative intensities of these dips, their wavenumber positions, and their widths are very comparable in both spectra in Fig. 6. When viewing the entire sweep, a substantial amount of apparent intensity noise can be observed on the swept QCL spectrum. However, zooming in on the time axis (see the inset in Fig. 6) shows that most of the apparent noise deviation results from systematic variations due to incomplete cancellation of the mode hops between the two detectors. Better matching of the two detectors will help to suppress these fluctuations. The water vapor absorption has been more successfully cancelled, by using the reference detector, in the spectrum taken by the external cavity laser. In the FTIR spectrum there are a few noticeable artefacts at the

Optics EXPRESS

wavenumber positions of the water vapor absorption, with the strongest ones being at ~1539, 1542, 1560 and 1616 cm^{-1}. They remain visible even after taking a reference spectrum through an empty cuvette. The slight discrepancy in the overall transmission signals in the two spectra can be explained either by a small difference in the acetophenone film thickness (the experiments were carried out at different times) or by some distortion of the non-collimated FTIR light beam, after positioning the transmission cell in the sample compartment of the FTIR spectrometer.

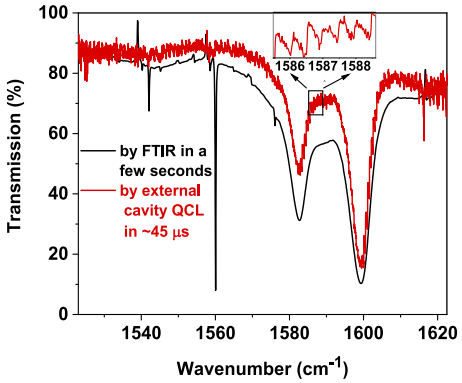

Fig. 6. The transmission spectra of a ~10-µm thick acetophenone liquid film measured through ~45 µs sweep time of the external cavity QCL (red curve) and by an FTIR spectrometer (black curve) with the resolution of 0.5 cm^{-1}. Inset plot: incomplete cancellation of the laser mode hops between the two detectors. Even after normalization using a reference from an empty cuvette, some remaining water vapor absorption features are still present in the spectrum measured with an FTIR spectrometer. Water vapor cancellation is more accurate using the QCL-based arrangement.

4. Discussion

To further exploit the ultimate speed limit for a CW external cavity QCL with a polygon mirror, a polygon scanner with a faster rotation speed can be introduced. For example, Precision Laser Scanning, LLC recently announced the fastest scanner commercially available, rotating at 70,000 RPM [24]. The sweep repetition rate can also be increased if a polygon mirror with a higher number of facets (for example, 36 facets for a similar diameter polygon mirror) is used. In our current system, only a small part of the polygon mirror facet is used to obtain feedback from the diffraction grating during the wavenumber sweep, so the laser is idle for ~82% of time. Hence, the use of a shorter mirror facet would lead to a higher duty cycle. As a result, the sweep repetition rate of a QCL, operating in the external cavity with a polygon mirror, can potentially be increased up to 40 kHz, which is one order more than of the present external cavity QCL systems with an oscillating MEOMS grating/mirror. The time for a sweep can be reduced by decreasing the groove density of a diffraction grating, however, with associated trade-offs in other areas, especially diffraction grating filter resolution and hence laser linewidth.

To fully realize the potential speed and resolution advantage of CW mid-infrared swept lasers, all sources of noise must be addressed. As it is clear from our results, CW swept lasers can suffer from high levels of relative intensity noise. The control of these fluctuations in the output intensity, which in our device are dominated by mode hops between the chip FP modes, is therefore an important design goal. The facet reflectivity in the QCL chip and careful attention to the desired diffraction grating filter resolution is an obvious area for improvement. It should allow to move from operation on the chip FP modes to operation on the modes of the external cavity, where the switching between much more closely spaced modes is expected to result in

Optics EXPRESS

lower laser intensity noise. The use of a tilted laser ridge facet [25] with or without an additional anti-reflection coating, would also lead to a dramatic decrease of the facet reflectivity. Positioning the external cavity laser set-up in a water vapor free enclosure should further help to minimize the intensity instabilities resulted from the water absorption influence. On the next level of improvement for the intensity stability and the wavenumber sweep-to-sweep stability at high RPMs of a rotating scanner, mechanical vibrations should also be controlled.

This work, and related developments in external cavity swept lasers, potentially allow the collection of high-quality spectra but in a fraction of the time required by an FTIR device. In part, this arises because collecting infrared spectra in the time-domain, rather than the Fourier-domain (as an FTIR device does), yields a fundamental signal-to-noise (SNR) advantage. Specifically, the same spectral SNR can theoretically be achieved in an acquisition time ×N shorter, given identical received optical power and detector noise [15]. This SNR advantage has long been recognized in the closely related area of near infrared OCT, where the switch from an FTIR-type readout of the OCT interferometer to a swept laser readout has been credited with a major boost in clinical applications [26]. Indeed, the polygon-scanner external cavity near infrared laser was the first commercially viable OCT swept laser (Santec, Japan) and research devices, using up to 16 stages of optical buffering, achieved sweep repetition rates up to 400 kHz [27].

5. Conclusions

The fast swept continuous wave room temperature quantum cascade laser operating in an external cavity with a rotating polygon mirror has been demonstrated. The sweeping time is less than ~45 µs for the wavenumber tuning range of ~1520 - 1625 cm^{-1}, the wavenumber resolution is better than 0.5 cm^{-1} and the sweep-to-sweep wavenumber stability is better than 0.018 cm^{-1}. The laser is constructed purely from catalogue components and, following further improvements, may be an ideal tool for high-quality mid-infrared spectral assessment of samples requiring fast acquisition times. The measurements of infrared transmission of a 10 µm thick layer of acetophenone liquid have demonstrated the capability of obtaining spectral data in less than 45 µs. The high speed and high spatial coherence of the source make it potentially well matched to applications such as hyperspectral imaging.

Funding. Engineering and Physical Sciences Research Council (EP/S025944/1).

Disclosures. The authors declare no conflicts of interest.

Data availability. Data underlying the results presented in this paper are available in Ref. [28].

References

1. J. Wagner, R. Ostendorf, J. Grahmann, A. Merten, S. Hugger, J.-P. Jarvis, F. Fuchs, D. Boskovic, and H. Schenk, "Widely tunable quantum cascade lasers for spectroscopic sensing," Proc. SPIE **9370**, 937012 (2015).
2. R. Ostendorf, L. Butschek, S. Hugger, F. Fuchs, Q. Yang, J. Jarvis, C. Schilling, M. Rattunde, A. Merten, J. Grahmann, D. Boskovic, T. Tybussek, K. Rieblinger, and J. Wagner, "Recent Advances and Applications of External Cavity-QCLs towards Hyperspectral Imaging for Standoff Detection and Real-Time Spectroscopic Sensing of Chemicals," Photonics **3**(2), 28 (2016).
3. C. S. Goldenstein, R. M. Spearrin, J. B. Jeffries, and R. K. Hanson, "Infrared laser absorption sensing for combustion gases," Prog. Energy Combust. Sci. **60**, 132–176 (2017).
4. C. Kumar N. Patel, "Single snapshot standoff detection using sub microsecond tuning speed quantum cascade lasers," Proc. SPIE **9836**, 98362E (2016).
5. C. S. Colley, J. C. Hebden, and D. T. Delpy, "Mid-infrared optical coherence tomography," Rev. Sci. Instrum. **78**(12), 123108 (2007).
6. N. M. Israelsen, C. R. Petersen, A. Barh, D. Jain, M. Jensen, G. Hannesschlager, P. Tidemand-Lichtenberg, C. Pedersen, A. Podoleanu, and O. Bang, "Real-time high-resolution mid-infrared optical coherence tomography," Light: Sci. Appl. **8**(1), 11 (2019).
7. C. Gmachl, A. Straub, R. Colombelli, F. Capasso, D. L. Sivco, A. M. Sergent, and A. Y. Cho, "Single-mode, tunable distributed-feedback and multiple-wavelength quantum cascade lasers," IEEE J. Quantum Electron. **38**(6), 569–581 (2002).

Optics EXPRESS

8. B. G. Lee, M. A. Belkin, R. Audet, J. MacArthur, L. Diehl, C. Pflügl, F. Capasso, D. C. Oakley, D. Chapman, A. Napoleone, D. Bour, S. Corzine, G. Höflerg, and J. Faist, "Widely tunable single-mode quantum cascade laser source for mid-infrared spectroscopy," Appl. Phys. Lett. **91**(23), 231101 (2007).
9. A. K. Goyal, M. Spencer, O. Shatrovoy, B. G. Lee, L. Diehl, C. Pfluegl, A. Sanchez, and F. Capasso, "Dispersion-compensated wavelength beam combining of quantum-cascade-laser arrays," Opt. Express **19**(27), 26725–26732 (2011).
10. R. Maulini, M. Beck, J. Faist, and E. Gini, "Broadband tuning of external cavity bound-to-continuum quantum-cascade lasers," Appl. Phys. Lett. **84**(10), 1659–1661 (2004).
11. A. Hugi, R. Terazzi, Y. Bonetti, A. Wittmann, M. Fischer, M. Beck, J. Faist, and E. Gini, "External cavity quantum cascade laser tunable from 7.6 to 11.4 μm," Appl. Phys. Lett. **95**(6), 061103 (2009).
12. G. Wysocki, R. F. Curl, F. K. Tittel, R. Maulini, J. M. Bulliard, and J. Faist, "Widely tunable mode-hop free external cavity quantum cascade laser for high resolution spectroscopic applications," Appl. Phys. B **81**(6), 769–777 (2005).
13. T. Tsai and G. Wysocki, "External-cavity quantum cascade lasers with fast wavelength scanning," Appl. Phys. B **100**(2), 243–251 (2010).
14. S. Hugger, F. Fuchs, J. Jarvis, M. Kinzer, Q. K. Yang, R. Driad, R. Aidam, and J. Wagner, "Broadband-tunable external-cavity quantum cascade lasers for the spectroscopic detection of hazardous substances," Proc. SPIE **8631**, 86312I (2013).
15. D. T. D. Childs, R. A. Hogg, D. G. Revin, I. U. Rehman, J. W. Cockburn, and S. J. Matcher, "Sensitivity advantage of QCL tunable-laser mid-infrared spectroscopy over FTIR spectroscopy," Appl. Spectrosc. Rev. **50**(10), 822–839 (2015).
16. B. E. Brumfield, M. S. Taubman, J. D. Suter, and M. C. Phillips, "Characterization of a swept external cavity quantum cascade laser for rapid broadband spectroscopy and sensing," Opt. Express **23**(20), 25553–25569 (2015).
17. A. Lyakh, R. Barron-Jimenez, I. Dunayevskiy, R. Go, E. Tsvid, C. Kumar, and N. Patel, "Progress in rapidly-tunable external cavity quantum cascade lasers with a frequency-shifted feedback," Photonics **3**(2), 19 (2016).
18. J. Xuefeng, W. Lijun, J. Zhiwei, Z. Ning, Z. Jinchuan, Z. Shenqiang, L. Junqi, L. Shuman, L. Fengqi, and W. Zhanguo, "Fast swept-wavelength, low threshold-current, continuous-wave external cavity quantum cascade laser," Nanoscale Res. Lett. **13**(1), 341 (2018).
19. V.- F. Duma, "Analysis of polygonal mirror scanning heads: from industrial to high-end applications in swept sources for OCT," Proc. SPIE **10056**, 100560P (2017).
20. S. H. Yun, C. Boudoux, G. J. Tearney, and B. E. Bouma, "High-speed wavelength-swept semiconductor laser with a polygon-scanner-based wavelength filter," Opt. Lett. **28**(20), 1981–1983 (2003).
21. B. Johnson, W. Atia, M. Kuznetsov, B. D. Goldberg, P. Whitney, and D. C. Flanders, "Analysis of a spinning polygon wavelength swept laser," arXiv:1501.07003v2 (2015).
22. J. A. Izatt, M. D. Kulkarni, H.-W. Wang, K. Kobayashi, and M. V. Sivak, "Optical coherence tomography and microscopy in gastrointestinal tissues," IEEE J. Sel. Top. Quantum Electron. **2**(4), 1017–1028 (1996).
23. A. Gambi, S. Giorgianni, A. Passerini, R. Visinoni, and S. Ghersetti, "Infrared studies of acetophenone and its deuterated derivatives," Spectrochim. Acta **36**(10), 871–878 (1980).
24. https://www.osa.org/en-us/about/newsroom/corporate_member_news/2016/precision_laser_scanning_announces_world_s_fastest/ (Accessed in December 2021).
25. W. Kideout, R. Holmstrom, J. Lacourse, E. Meland, and W. Powazinik, "Ultra-low-reflectivity semiconductor optical amplifiers without antireflection coatings," Electron. Lett. **26**(1), 36–38 (1990).
26. M. A. Choma, M. V. Sarunic, C. Yang, and J. A. Izatt, "Sensitivity advantage of swept source and Fourier domain optical coherence tomography," Opt. Express **11**(18), 2183–2189 (2003).
27. W.-Y. Oh, B. J. Vakoc, M. Shishkov, G. J. Tearney, and B. E. Bouma, ">400 kHz repetition rate wavelength-swept laser and application to high-speed optical frequency domain imaging," Opt. Lett. **35**(17), 2919–2921 (2010).
28. D. Revin and S. Matcher, "Dataset for "Fast-sweeping continuous wave quantum cascade laser operating in an external cavity with polygon mirror"," The University of Sheffield Research Data Repository (2022), https://doi.org/10.15131/shef.data.19251686.v1